EVOLUTION OF RADIATION POWER PROFILES IN ASDEX H-MODE DISCHARGES

E. R. Müller[1], C. Janeschitz, P. Smeulders[1], G. Fussmann, M. Kornherr, K. F. Mast, G. Becker, H. S. Bosch, H. Brocken, A. Eberhagen, O. Gehre, J. Gernhardt, G.v.Gierke, E. Glock, O. Gruber, G. Haas, J. Hofmann, A. Izvozchikov[2], F. Karger, M. Keilhacker[1], O. Klüber, K. Lackner, M.Lenoci, G. Lisitano, H. M. Mayer, K. McCormick, D. Meisel, V. Mertens, H. Murmann, H. Niedermeyer, A. Pietrzyk[3], W. Poschenrieder, H. Rapp, H. Riedler, H. Röhr, J. Roth, F. Ryter[4], F. Schneider, C. Setzensack, G. Siller, F. X. Söldner, E. Speth, K.-H. Steuer, O. Vollmer, F. Wagner, D. Zasche

Max-Planck-Institut für Plasmaphysik
EURATOM Association, D-8046 Garching

Abstract

The paper compares the impurity radiation behaviour of two types of H-mode discharges. In the normal H-mode that reaches a quasi-stationary state the energy (and particle) losses within the outer plasma half-radius are characterized by the repetitive burst-like exhaust into the divertor and constantly moderate radiation power losses. In contrast, the burst-free variant of the H-mode with superior confinement properties is dominated by radiation losses growing continuously up to 100 % of the heating power. The time evolution of the impurity concentration and the associated radiation losses at the plasma centre is hardly influenced by the kind of H-mode. If the concentration of medium-heavy metals in the burst-dominated H-mode plasma is raised to sufficiently high values, e.g. by the accumulation of intrinsic iron, the burst-free (or burst-deficient) H-mode is triggered which after a new accumulation period usually ends by a radiation collapse.

1. Introduction

During the normal H-mode /1/ of neutral-injection heated divertor discharges in the tokamak ASDEX the energy and particle flow from the main plasma volume into the divertor is modulated by highly repetitive bursts. While typical bursts exhibit pulse lengths of around 0.5 ms and power amplitudes of the order of 1 MW, the energy exhaust into the divertor is almost blocked during the quiescent intervals between bursts /2/.

In order to investigate the influence of the bursts, a discharge with a long-lasting burst-free H-mode (shot # 11447) has been produced /3/ and is contrasted with that kind of H-mode endowed with the usual burst-pattern (shot # 11338). Both discharges have identical parameter settings at the beginning of the NI-heating interval (I_p = 320 kA, B_t = 2.17 T, $\bar{n}_e$ = 3.5 x 10^{13} cm^{-3}, $P_{OH} + P_{NI}$ = 3.3 MW, $H^0 \rightarrow D^+$ (40 kV) tangential injection in co-direction) except for the 4 cm outward shift of the plasma needed to establish the long-lasting burst-free H-phase. The time history of various plasma parameters ($\bar{n}_e$, β_p, τ_E^* etc.) is discussed in Ref. /3/.

Figure 1 shows that the bolometrically measured total volume power losses within the divertor (RAD_{DIV}) /4/ drop instantly at the L-to-H mode transition (t = 1.16 s) and remain at the low level of the ohmic phase throughout the burst-free H-mode, whereas they recover time-averaged over the bursts

---

[1]Present address: JET Joint Undertaking, Culham, England; [2]Academy of Sciences, Leningrad, USSR; [3]Univ. of Washington, Seattle, USA; [4]CEN Grenoble, France

with growing burst activity during the second variant of H-mode. The total radiation power losses of the main plasma volume (RAD) are considerably higher in the burst-free H-discharge, even during the preceding L-phase. This radiation enhancement indicates an impurity contamination of the plasma produced by its shift to the outer stainless-steel protection limiters. The burst-free H-mode is terminated when, after a continuous radiation increase accelerated by a simultaneous rise of plasma density, the value of the main plasma radiation (RAD) equalizes the total heating power.

2. Radiation power profiles

Figure 2 compares the two types of H-mode discharges at two discrete times with regard to their chord-intensity profiles measured with a 19-bolometer array, and Fig. 3 presents the time development of the respective radial profiles of radiation power density ($P_{RAD}(r)$) derived by Abel-inversion method. During each kind of H-mode the radiation profiles evolve towards shapes peaked at the plasma centre. The repetitive burst-like release of plasma energy due to the Edge Localized Modes (ELMs) /3,5/ prevents any long-term increase of radiation power at plasma radii between a/2 and a. In this case, the growth of the central radiation peak is restricted to the inner half-radius and at t = 1.260 s it is reversed into a decay towards an equilibrium profile identical to that at t = 1.215 s. In contrast, during the burst-free H-mode, where the energy outflow into the divertor is permanently suppressed, the radiation power losses grow unimpeded over nearly the whole plasma cross-section until the radiation collapse converts the discharge back into the L-mode. The burst activity and the radiation enhancement thus act mutually exclusively as additional important energy loss mechanisms within the outer plasma half-radius and, depending on the class of H-mode, both quantitatively substitute each other. The main plasma radiation becomes the dominant energy loss channel in the burst-free H-mode. Therefore, the energy flow into the divertor (see e.g. RAD_{DIV} signal in Fig. 1) keeps low and does not restore the previous L-mode level as one would expect for transport-dominated losses after the plasma equilibrium (with improved confinement) is re-established.

It is important to note that the chord-intensity profile of the burst-dominated H-mode which ends up quasi-stationary stays always, even during its transient central peaking, distinctly below the base profile from which the fatal radiation increase of the burst-free H-mode starts at t=1.215s (Fig.2).

3. Radiation and impurity accumulation at the plasma centre

Correlation of the bolometric radiation profiles (Fig. 3) with those from VUV spectroscopy, soft X-ray tomography, temperature and density measurements makes evident that the radiation emission at the plasma centre is completely dominated by line radiation of highly ionized iron /3/ and that the central peaking of the radiation profiles reflects an impurity accumulation taking place irrespective of the type of H-mode. Figure 4 demonstrates that the presence or absence of bursts hardly influences the evolution in time of the local radiation power density at the plasma centre ($P_{RAD}(0)$), particularly the time-constant of the exponential rise after the L-to-H-mode conversion. The absolute magnitude of $P_{RAD}(0)$, however, is at any instant, including the preceding L-phase, about three times higher in the burst-free H-discharges as compared with the burst-dominated one, due to the initial iron contamination. The iron concentration at the plasma centre, displayed in Fig. 5, is derived from $P_{RAD}(0)$ by applying the temperature-dependent radiative power loss function for iron $P_{Fe}(T_e)$ /6/, that includes charge-exchange recombination with beam neutrals ($n_o/n_e = 10^{-5}$).

4. Internal triggering of the burst-free H-mode

Shot # 12218 (Figs. 6 and 7) shows that the burst-dominated H-mode with moderate radiation losses may turn into the burst-deficient H-mode with disastrous consequences. The mode conversion occurs when the accumulation of intrinsic metal impurities during the burst-dominated H-phase raises the bolometric centre-chord intensity up to the threshold value of the burst-deficient H-mode. The first and the last step in the profile evolution depicted in Fig. 7 resemble strikingly their burst-dominated and burst-free counter-parts in Fig. 2, respectively, because the burst frequency in the burst-deficient H-mode seems to be too low to slow down the impurity accumulation. Our interpretation that a sufficient degree of plasma contamination with medium-heavy metals is needed to establish the long-lasting burst-free H-mode agrees with the experimental observation that the burst-free H-mode can be triggered externally by the laser blow-off injection of metals such as chromium and copper /7/.

References:

/1/ Wagner, F., et al., Phys. Rev. Lett. 49 (1982) 1408.
/2/ Müller, E.R., et al., Journ. Nucl. Mat. 121 (1984) 138.
/3/ Keilhacker, M., et al., in Plasma Physics and Contr. Nuclear Fusion Res. (Proc. 10th Int. Conf. London, 1984) Vol.1, IAEA, Vienna (1985) 71.
/4/ Müller, E.R., Behringer, K., Niedermeyer, H., Nucl. Fus. 22 (1982) 1651.
/5/ Wagner, F., et al., Phys. Rev. Lett. 53 (1984) 1453.
/6/ Hulse, R.A., Post D.E., Mikkelsen, D.R., J. Phys. B: Atom. Molec. Phys. 13 (1980) 3895.
/7/ Keilhacker, M., et al., Plasma Phys. and Contr. Fusion, 28, (1986) 29.

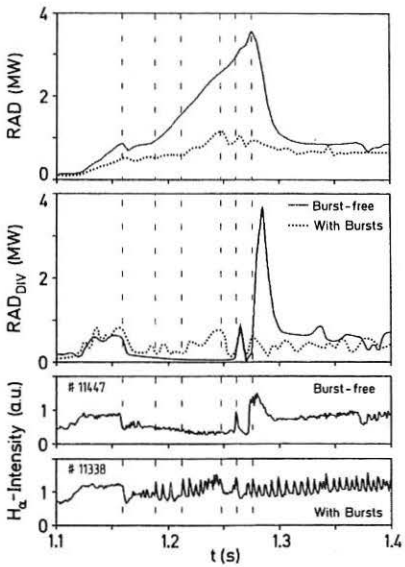

Fig. 1 (left): Time history of the bolometer signals RAD and RAD$_{DIV}$ (electronic integration-time ≈10 ms) for both kinds of H-mode discharges.

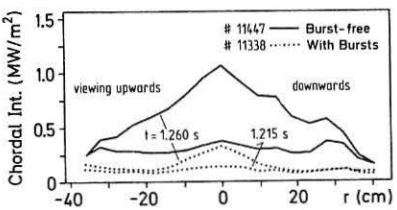

Fig. 2 (above): The bolometric chord-intensity profiles characteristic of either type of H-mode at two discrete times.

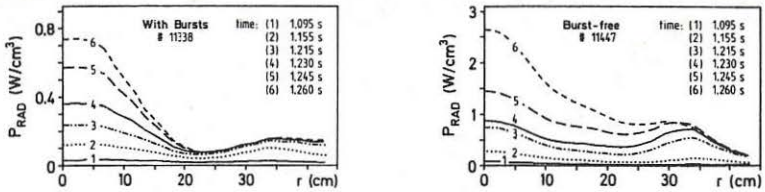

Fig.3: Time evolution of the radial profile of radiation power density during the burst-dominated (left) and the burst-free (right) H-mode discharge (note the different radiation scales).

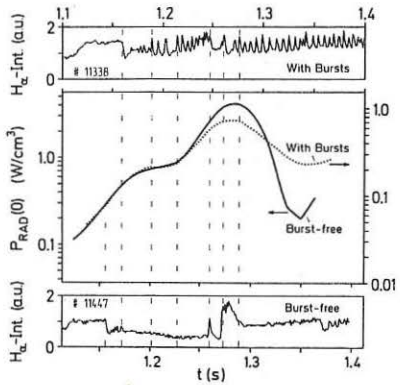

Fig. 4: Dynamic behaviour of the radiation power densities at the plasma centre.

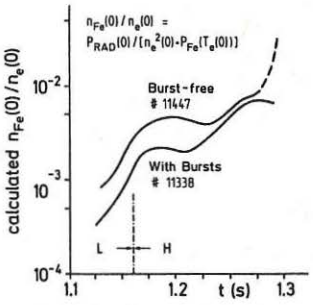

Fig. 5: Variation in time of the calculated iron concentrations at the plasma centre.

Fig. 6 (right): Time development of various plasma parameters during shot #12218 converting from a burst-dominated into a burst-deficient H-mode.

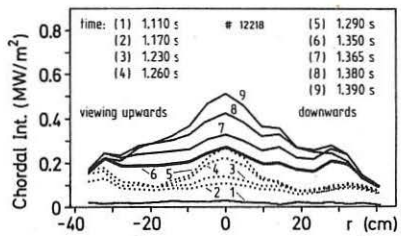

Fig. 7 (above): The evolution of the bolometric chord-intensity profile during shot #12218.